

# Using Cell Membranes as Recognition Layers to Construct Ultrasensitive and Selective Bioelectronic Affinity Sensors

Eva Vargas, Fangyu Zhang, Amira Ben Hassine, Victor Ruiz-Valdepeñas Montiel, Rodolfo Mundaca-Uribe, Ponnusamy Nandhakumar, Putian He, Zhongyuan Guo, Zhidong Zhou, Ronnie H. Fang, Weiwei Gao, Liangfang Zhang\*, and Joseph Wang\*



Cite This: *J. Am. Chem. Soc.* 2022, 144, 17700–17708



Read Online

ACCESS |

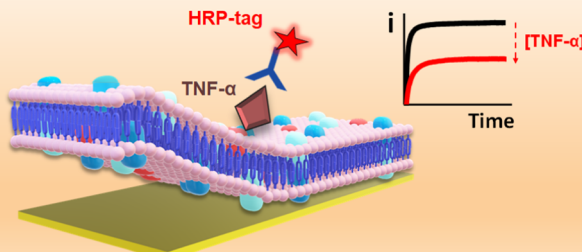
Metrics & More

Article Recommendations

Supporting Information

**ABSTRACT:** Conventional sandwich immunosensors rely on antibody recognition layers to selectively capture and detect target antigen analytes. However, the fabrication of these traditional affinity sensors is typically associated with lengthy and multistep surface modifications of electrodes and faces the challenge of nonspecific adsorption from complex sample matrices. Here, we report on a unique design of bioelectronic affinity sensors by using natural cell membranes as recognition layers for protein detection and prevention of biofouling. Specifically, we employ the human macrophage (MΦ) membrane together with the human red blood cell (RBC) membrane to coat electrochemical transducers through a one-step process. The natural protein receptors on the MΦ membrane are used to capture target antigens, while the RBC membrane effectively prevents nonspecific surface binding. In an attempt to detect tumor necrosis factor alpha (TNF- $\alpha$ ) cytokine using the bioelectronic affinity sensor, it demonstrates a remarkable limit of detection of 150 pM. This new sensor design integrates natural cell membranes and electronic transduction, which offers synergistic functionalities toward a broad range of biosensing applications.

## Cell Membrane based-Bioelectronic Affinity Sensor



## 1. INTRODUCTION

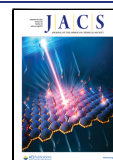
The development of rapid and reliable analytical techniques for detecting key disease biomarkers in complex biological samples attracts tremendous attention. Immunoassays have been particularly useful for detecting different biological molecules for diverse applications due to their inherent high sensitivity and selectivity.<sup>1–3</sup> These affinity-based assays rely on the highly selective interaction between antibody receptors and target antigens through specific molecular recognition domains.<sup>4</sup> Conventional immunoassays are based on sandwich assay formats, involving the binding of two antibodies to different regions of the target analyte. These devices include a capture antibody that is confined to the transducer surface and a detection antibody that is usually tagged with an enzyme for converting the specific recognition event into a physically detectable electronic or optical signal.<sup>5–7</sup> Integrating the capture antibody receptor with the signal transduction is usually accomplished by modifying the transducer surface with a chemical reagent layer.<sup>8</sup> The fabrication of electrochemical immunoassays involves lengthy stepwise protocols for achieving proper surface chemistry toward optimal confinement of the capture antibody on the electrode transducer and efficient antigen binding while preventing nonspecific adsorption from complex sample

matrices. Such surface preparation procedure hinders the scalable manufacturing of bioelectronic immunoassays.<sup>9</sup> Furthermore, the design of immunoassays is often limited by the lack of commercially available antibodies specific to certain target analytes. In this context, other biological entities such as aptamers, peptides, proteins, cell microsomes, or even whole cells with selective biorecognition domains have received growing attention toward the development of affinity sensors for detecting a wide range of targets.<sup>4,8,10,11</sup>

Here, we report on a new bioelectronic affinity sensing strategy that incorporates natural cell membranes as recognition layers, as an attractive alternative to antibody receptors in conventional immunoassays. Cell membrane coating technology constitutes a robust top-down strategy for replicating the rich biological functionalities of cellular membranes on synthetic materials or devices.<sup>12–15</sup> The natural cell membrane coating retains membrane proteins and lipids,

Received: July 27, 2022

Published: September 16, 2022



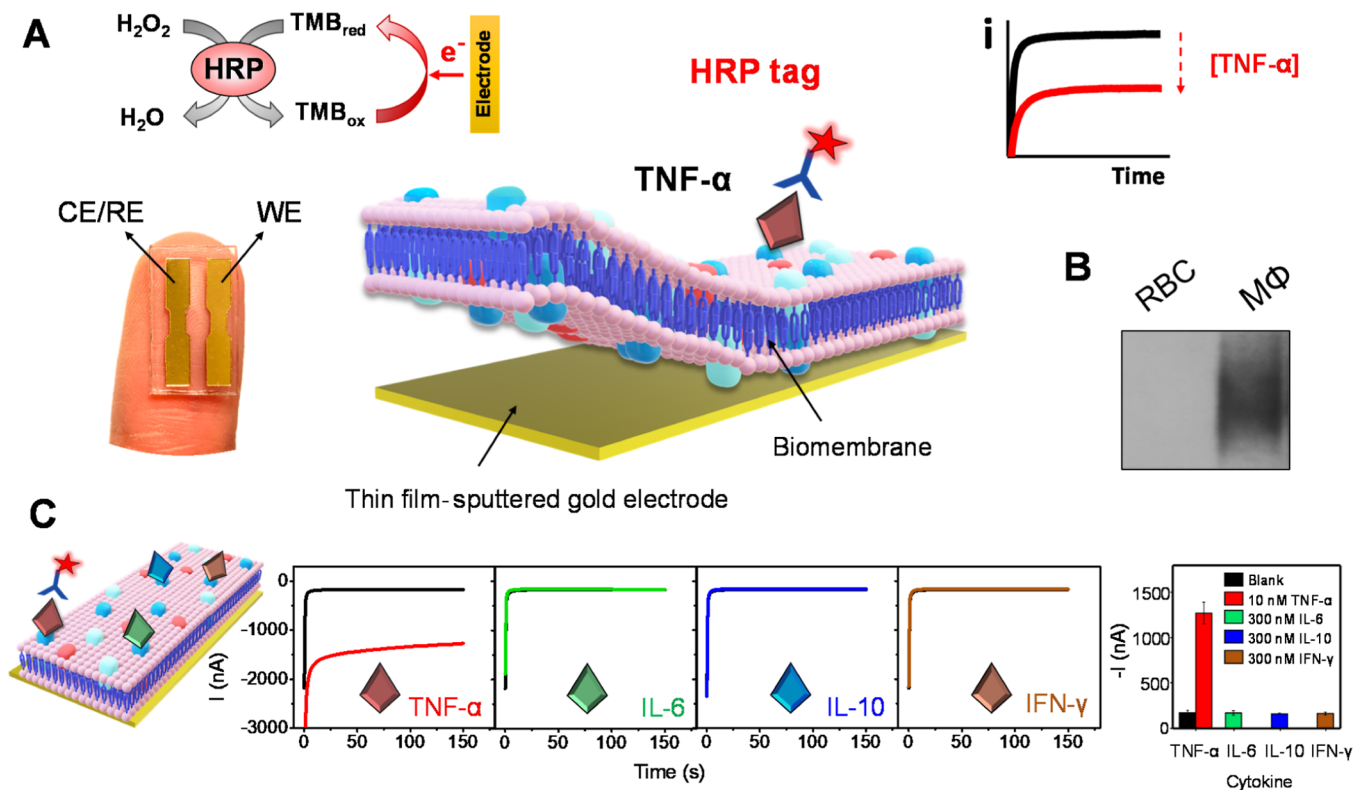


**Figure 1.** Cell membrane-based bioelectronic affinity sensor for TNF- $\alpha$  detection. (A) Schematic illustration of the cell membrane-based sensor including a gold-electrode transducer (left) and macrophage (MΦ)/RBC hybrid membrane surface coating along with the use of HRP-tagged TNF- $\alpha$  antibody and TMB-based amperometric detection (center). (B) Western blot analysis showing the presence of TNF- $\alpha$  receptor (TNF $\alpha$ R1) on the MΦ membrane but not on the RBC membrane. (C) Evaluation of the specificity of the cell membrane-based sensor in response to different cytokines.

and thus bestows the coated devices with unique properties to interface with biological systems, including capture and isolation of biological targets and prevention of nonspecific adsorption.<sup>16–18</sup> Cell membranes have been derived from various cell types, such as platelets,<sup>14</sup> macrophages,<sup>13</sup> cancer cells,<sup>12</sup> erythrocytes,<sup>15</sup> and leukocytes.<sup>19</sup> The coating has been achieved through procedures such as extrusion, homogenization, or sonication.<sup>20</sup> Cell membranes were used recently to functionalize field effect transistors for capture and detection of bacteria and toxins using the red blood cell (RBC) membrane coating technology.<sup>21</sup>

In this work, we derived macrophage cell membranes, coated them onto electrochemical transducers, and examined their performance in detecting membrane affinity biomolecules (Figure 1A). We chose tumor necrosis factor-alpha (TNF- $\alpha$ ) as a model analyte due to its significant role in numerous inflammatory diseases.<sup>22,23</sup> In this biomimetic platform, the specific detection of TNF- $\alpha$  relied on the natural TNF- $\alpha$  receptors on the macrophage membrane recognition layer and a horseradish peroxidase (HRP)-tagged anti-TNF- $\alpha$  detection antibody (HRP-Ab). To prevent nonspecific binding, we further fused the macrophage membrane with the RBC membrane and used the hybrid membrane to functionalize the transducers. Specifically, a gold electrode chip functionalized with the hybrid cell membrane was used for single sample incubation-based TNF- $\alpha$  affinity assays, in which the target cytokine was selectively captured by the cell membrane TNF- $\alpha$  receptors and then tagged with the HRP-Ab (Figure S1 in Supporting Information). This sandwich-like cell-membrane assay employed 3,3',5,5'-tetramethylbenzidine (TMB)/H<sub>2</sub>O<sub>2</sub>

as the mediator/substrate redox detection system. In the presence of the target TNF- $\alpha$ , the captured HRP enzyme catalyzes the oxidation of TMB with the support of H<sub>2</sub>O<sub>2</sub>, and the oxidized TMB returns to its original state by the electrochemical reduction reaction. The observing reduction currents directly relate to the HRP-Ab captured on the sensor surface and are directly proportional to the level of the target TNF- $\alpha$ . Common colorimetric assay of TMB/HRP/H<sub>2</sub>O<sub>2</sub> needs several minutes to oxidize the TMB in bulk solution to differentiate the blank and target TNF- $\alpha$ ; however, in amperometry, the oxidized TMB is selectively reduced upon applying a constant potential ( $-0.1$  V) for 150 s. During such detection, HRP-Ab bound on the sensor surface rapidly oxidizes the TMB, and it further contributes to the electrochemical signal. A stable and chemical-free capture recognition film was easily prepared by the simple dropcasting of cell membrane solution on the bare electrode surface, obviating the need for functional linking groups or complex and tedious surface treatment and functionalization steps common to conventional immunosensors. Additionally, the uniform biomembrane layer minimizes the nonspecific adsorption of enzyme-tagged antibodies on the electrode, obviating the need for additional surface blocking steps. The presence of TNF- $\alpha$  receptor on macrophage membrane was verified by Western blot analysis (Figure 1B). The sensor operation led to ultrasensitive and selective detection of 10 nM TNF- $\alpha$  with a negligible response from a large excess (300 nM) of other cytokines (Figure 1C) and enabled detection down to 500 pM TNF- $\alpha$ , which will be demonstrated in the following sections.

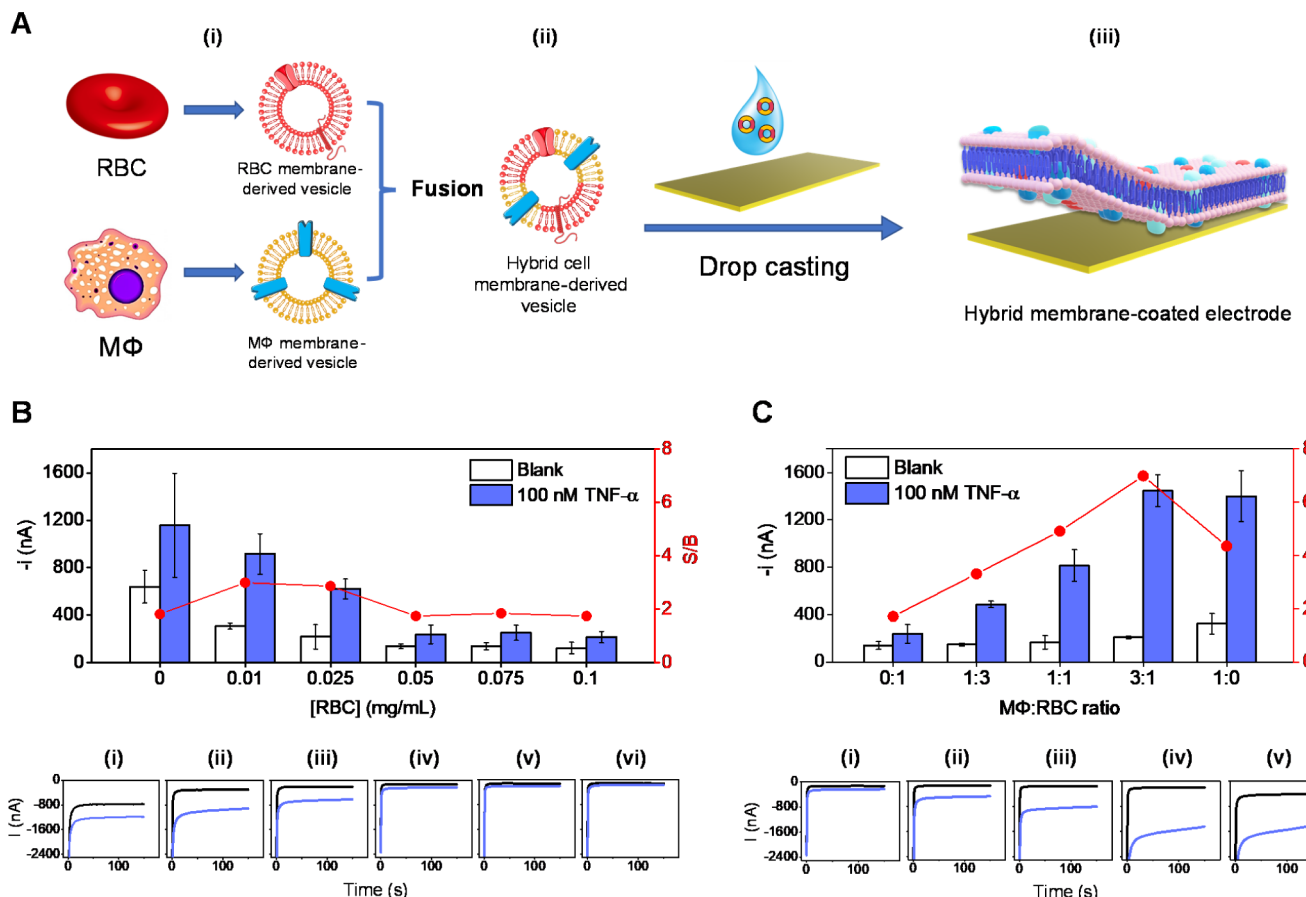


**Figure 2.** Fabrication and optimization of MΦ/RBC hybrid membrane-coated bioelectronic sensor chips. (A) Schematic fabrication of MΦ/RBC hybrid membrane-coated bioelectronic platform: preparation of RBC and MΦ membrane-derived vesicles (i); formation of hybrid cell membrane vesicles through a fusion process (ii); subsequent coating of the hybrid vesicles on the sensor gold surface by drop casting (iii). (B) Optimization of the RBC membrane concentration toward minimized nonspecific adsorption: chronoamperometric responses and S/B ratios obtained with sensor chips uncoated (bare Au, 0 mg/mL RBC) and coated with RBC membrane at different concentrations (0.01–0.1 mg/mL) in the absence (white bars, “Blank”, “B”) and presence of 100 nM TNF- $\alpha$  standard (blue bars, “S”); (i–vi) representative signals corresponding to measurements of no TNF- $\alpha$  (black lines) and 100 nM TNF- $\alpha$  (blue lines) obtained for each RBC concentration. (C) Optimization of the MΦ/RBC hybrid membrane composition toward ultrasensitive TNF- $\alpha$  detection: chronoamperometric responses and S/B ratios obtained with sensor chips coated with hybrid membranes of different MΦ/RBC ratios in the absence (white bars, “Blank”, “B”) and presence of 100 nM TNF- $\alpha$  standard (blue bars, “S”); (i–v) representative signals corresponding to measurements of no TNF- $\alpha$  (black lines) and 100 nM TNF- $\alpha$  (blue lines) obtained for each hybrid membrane composition. Column bars and error bars represent the mean and the standard deviation from three replicas, respectively.

## 2. EXPERIMENTAL SECTION

Experimental details about instrumentation and reagents employed have been included in the *Supporting Information*.

**2.1. Cell Membrane Derivation and Hybridization.** The human RBC membrane was derived from RBCs using a previously described protocol.<sup>15</sup> Briefly, whole blood was first washed with 1× phosphate-buffered saline (PBS, Corning) containing 1 mM ethylenediaminetetraacetic acid (EDTA, Sigma-Aldrich) 3 times to remove the serum and buffy coat. Washed RBCs were then resuspended in 0.25× PBS and placed on ice for 20 min. Hemoglobin released in this hypotonic treatment was removed with centrifugation (8000g for 3 min at 4 °C). Purified RBC membranes were finally resuspended in 1× PBS containing 0.2 mM EDTA and stored in a –80 °C freezer. Meanwhile, the human macrophage membrane was derived from the THP-1 cell line based on a previously published protocol.<sup>24</sup> Specifically, THP-1 cells were grown in RPMI 1640 (Gibco) supplemented with 10% FBS and 1% penicillin-streptomycin. The cells were collected and washed with 1× PBS three times and then suspended in a hypotonic lysing buffer containing 30 mM Tris-HCl (pH = 7.5), 225 mM D-mannitol, 75 mM sucrose, 0.2 mM ethylene glycol-bis ( $\beta$ -aminoethyl ether)-(N,N,N',N'-tetraacetic acid) (EGTA), and protease and phosphatase inhibitor cocktails (all from Millipore-Sigma).

Cells were then disrupted using a Dounce homogenizer with a tight-fitting pestle (20 passes). The homogenized solution was centrifuged at 20,000g and 4 °C for 25 min. The pellet was discarded, and the supernatant was centrifuged again at 100,000g and 4 °C for 35 min. Following the centrifugation, the membrane was collected as the pellet and washed twice with 0.2 mM EDTA in water. Membrane content was quantified by using a BCA protein assay (Thermo Fisher Scientific). To fabricate the hybrid cell membrane, the RBC membrane and the macrophage membrane were mixed with different ratios and incubated at 37 °C for 15 min. The membrane mixture was then sonicated with a bath sonicator (Fisher Scientific FS30D) for 3 min to generate hybrid membrane-derived vesicles.

**2.2. Thin-Film Au-Sputtered Chips Fabrication.** The homemade chip fabrication procedure was based on a previously reported protocol.<sup>25</sup> The chips were manufactured as electrode arrays consisting of two Au-sputtered square electrodes (13.8 mm<sup>2</sup> area each) serving as the working electrode (WE) and as the joint reference/counter (RE/CE) electrode, respectively. The electrode substrates used in this protocol were 1 mm thick PETG (glycol-modified polyethylene terephthalate) plastic sheets from Small Parts Inc. The electrode design pattern was cut out of the substrates' protective laminated cover using a Cricut machine. Cr and Au metals were sputter coated by using a Denton Discovery 18 Sputter System

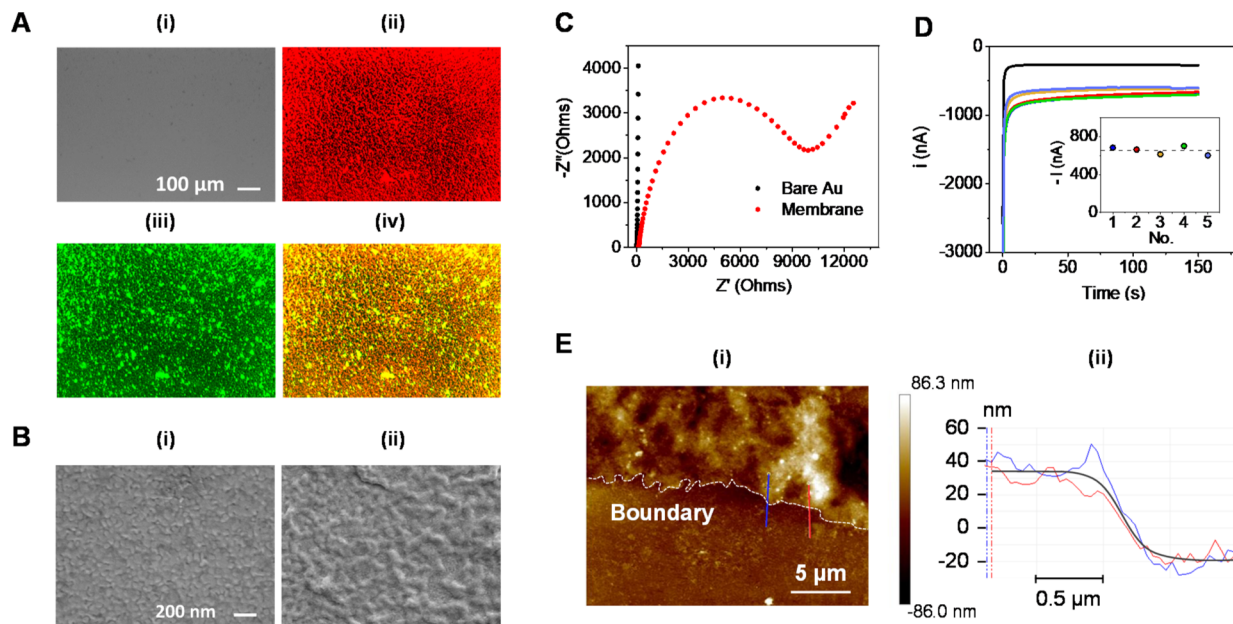


**Figure 3.** Characterization of hybrid cell membrane-coated bioelectronic sensor chips. (A) Fluorescence images of the hybrid cell membrane-coated gold electrode: (i) Bright field; (ii) RFP channel: Dil-labeled macrophage membrane; (iii) GFP channel: DiO-labeled RBC membrane; (iv) Merged. (B) SEM images of (i) bare gold electrode and (ii) gold electrode with 0.1 mg/mL hybrid membrane coating. (C) EIS measurements showing the hybrid membrane coating on Au chips (red curve) vs the bare Au (black curve). (D) Reproducibility of the membrane sensor fabrication—responses for 5 nM TNF- $\alpha$  at 5 different sensors prepared using the same fabrication protocol. (E) AFM analysis for coating thickness characterization: topography image (i) and corresponding line profiles of marked red and blue lines (ii).

under the direct current (DC) mode at 200 W for 20 s and 5 min for Cr and Au, respectively, under Ar gas pressure of 2.4 mTorr. Finally, the electrodes were simply cleaned by two 10 min washing steps by immersion in isopropyl alcohol and water, and dried with a compressed air gun before use.

**2.3. Cell Membrane-Coated Bioelectronic Chip Preparation and Characterization.** The hybrid membrane coating onto single chips was achieved by drop casting 30  $\mu$ L suspension of MΦ/RBC hybrid cell membrane vesicles (0.05 mg/mL, protein concentration) on the bare Au WE surface followed by overnight drying at room temperature. The resulting cell membrane-modified Au chips were stored at 4 °C for subsequent uses. Electrochemical impedance spectroscopy (EIS) experiments were performed in a 0.1 M KCl solution containing 5 mM  $[\text{Fe}(\text{CN})_6]^{3-}/4-$  at 0.22 V DC potential with 5 mV AC amplitude and frequencies ranging from 0.1 to 10<sup>5</sup> Hz. Scanning electron microscope (SEM) images of uncoated and cell membrane-coated gold chips were performed on a Zeiss Sigma 500 SEM instrument with an acceleration voltage of 3 kV. To verify membrane coating on the chip, RBC and macrophage membranes were labeled with a DiO (Thermo Fisher Scientific, excitation/emission = 484/501 nm) and DiI (Thermo Fisher Scientific, excitation/emission = 550 nm/567 nm) before membrane fusion. Following the process to make a hybrid cell membrane-coated chip, fluorescent imaging was performed to visualize the colocalization of two membranes under an Invitrogen EVOS FL fluorescence microscope with a 20× objective. The morphology and roughness of cell membrane coatings on gold chips were characterized by atomic force microscopy (AFM) in the contact mode using tips (Bruker, no. MLCT). Western blot was conducted to assess the presence of a specific protein marker on the macrophage membrane. Gels were transferred onto a nitrocellulose membrane (Thermo Scientific) and probed with antibodies (ab223352, Abcam) specific for human TNF- $\alpha$  Receptor I.

**2.4. TNF- $\alpha$  Bioassay Protocol.** To detect TNF- $\alpha$ , cell membrane-coated WE was incubated with a droplet of TNF- $\alpha$  solution (10  $\mu$ L). This solution was prepared either with TNF- $\alpha$  standard in 0.1 M PBB (phosphate buffer, pH 7.4, and containing 1% BSA), or in half-diluted human serum, and supplemented with 1  $\mu$ g/

mL of HRP-Ab (Figure S1). The WE was subsequently washed 3 times with PB solution and dried with compressed air. Finally, the TNF- $\alpha$  detection was performed by chronoamperometry using the H<sub>2</sub>O<sub>2</sub>/HRP/TMB redox probe for the transduction. Thus, a 20  $\mu$ L-drop of the commercial H<sub>2</sub>O<sub>2</sub>/TMB substrate/mediator solution was dropped onto the sensor chip covering both WE and RE/CE, and the amperometric signal was promptly recorded by applying a potential of −0.1 V for 2.5 min.

### 3. RESULTS AND DISCUSSION

**3.1. Fabrication and Optimization of the Hybrid Cell Membrane-Coated Sensor Chip.** The preparation of the cell membrane-based bioelectronic sensor chip consisted of three steps (Figure 2A). First, purified RBC and macrophage membranes were sonicated and fused to generate hybrid membrane vesicles. The hybrid membrane vesicles were then drop cast onto a Au-sputtered electrode using an adjusted volume of 30  $\mu$ L of vesicle suspension that allowed us to produce a uniform biomembrane coating localized on the working electrode area (without covering the reference electrode). Such a simple chemical-free protocol for functionalization of sensor chips with bioreceptors, along with the single incubation-based antigen detection (Figure S1), greatly facilitates scalable fabrication of the biosensor devices, which distinguishes from conventional immunoassays made through time-consuming multistep costly modification protocols. The synergistic functionality of the macrophage/RBC hybrid membrane was explored by adjusting the vesicle load and composition of the hybrid membrane coating. Nonspecific adsorption represents a major challenge for TNF- $\alpha$  detection and the accuracy of the biosensor considering that many serum proteins, including TNF- $\alpha$ , contain thiol groups and thus can bind nonspecifically to the sensor chip surface,<sup>26–29</sup> which could lead to false-positive signals (Figure S2). To inhibit the nonspecific binding, RBC membrane-derived vesicles were

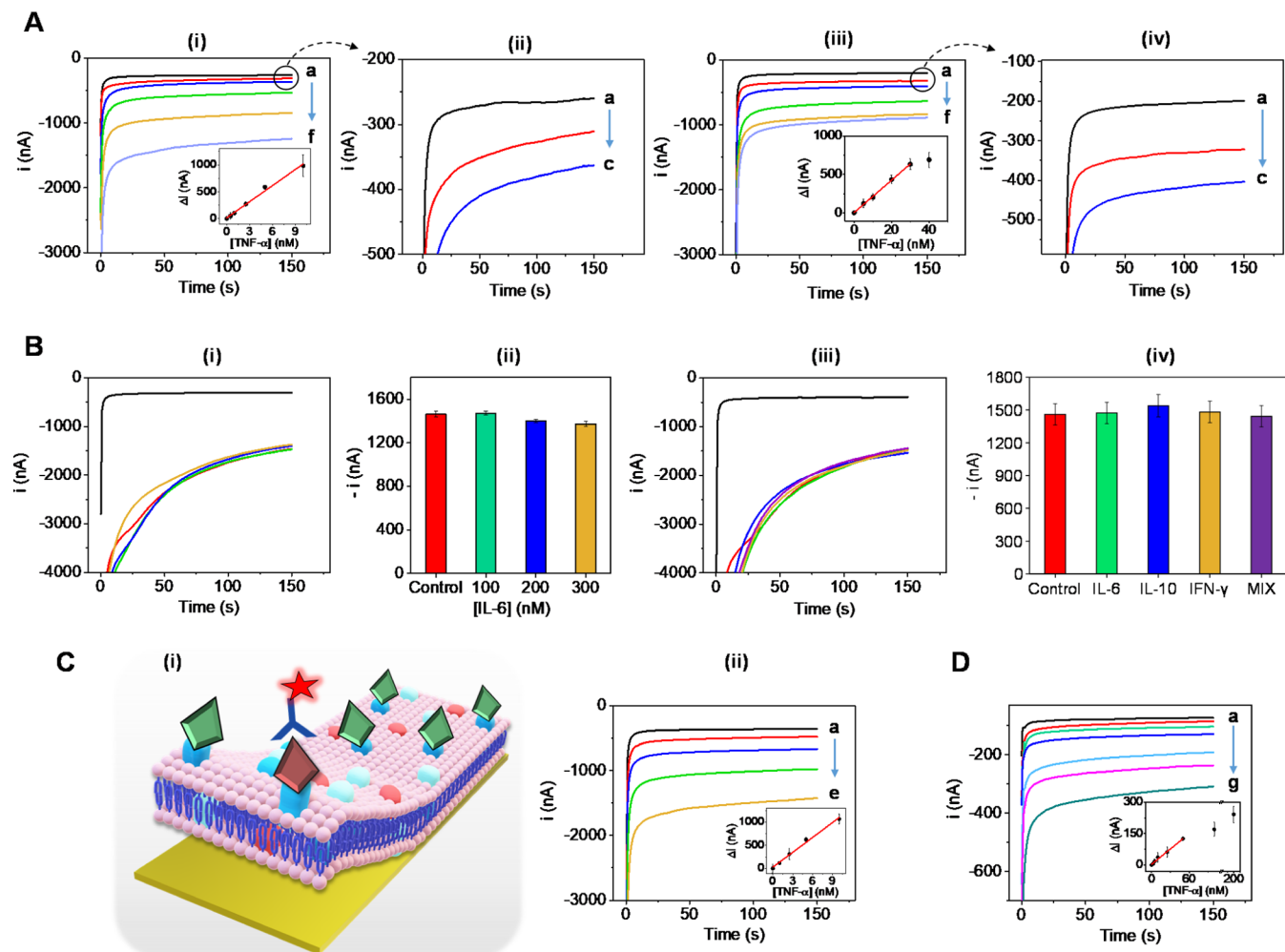


**Figure 4.** Analytical performance of cell membrane-coated bioelectronic sensor chips. (A) Calibrations for TNF- $\alpha$  in buffer solutions: (i) applying 20 min incubations—signals for 0, 0.5, 1, 2.5, 5, and 10 nM TNF- $\alpha$ ; (ii) zoom-in for 0, 0.5, and 1 nM TNF- $\alpha$ ; (iii) applying 5 min incubations signals for 0, 5, 10, 20, 30, and 40 nM TNF- $\alpha$ ; (iv) zoom-in for 0, 5, and 10 nM TNF- $\alpha$ . (B) Evaluation of the effect of high concentration of other cytokines upon the detection of 100 nM TNF- $\alpha$ : amperograms (i) and averaged responses (ii) obtained in the absence (“control”) and presence of increasing concentrations of IL-6; amperograms (iii) and averaged responses (iv) obtained in the absence (“control”) and presence of 100 nM of other cytokines and a mixture of all of them. (C) Efficient detection of TNF- $\alpha$ : (i) schematics representing measurements of a low amount of TNF- $\alpha$  in the presence of an excess of IL-6 and (ii) TNF- $\alpha$  calibration in buffer solutions in the presence of 50 nM IL-6 and detection of 1, 2.5, 5, and 10 nM TNF- $\alpha$ . (D) TNF- $\alpha$  calibration in half diluted human serum and detection of 2.5, 5, 10, 25, 50, 100, and 200 nM TNF- $\alpha$  in standard-spiked samples. Column bars and error bars represent the mean and the standard deviation from three replicas, respectively.

used to coat the electrode and achieve effective antibiofouling effects by optimizing the membrane load (Figure 2B). The level of nonspecific adsorption of the HRP-Ab and TNF- $\alpha$  protein on the gold surface was evaluated in PBB (phosphate buffer containing 1% BSA) solutions by chronoamperometry. Sensor chips uncoated and coated with different RBC membrane concentrations were tested in the absence and presence of a high concentration of TNF- $\alpha$ . A larger amount of membrane coated on the gold surface provided better protection against undesired protein adsorption. It was shown that 0.05 mg/mL (1.5  $\mu$ g) of membrane load reached the plateau of the signal-to-blank (S/B) ratio variation given by minimal attachment of both HRP-Ab and TNF- $\alpha$  protein. Additional experiments revealed that RBC membrane coating was able to effectively prevent nonspecific adsorption of various concentrations of TNF- $\alpha$  (Figure S2). Next, the composition of the two types of membranes was optimized to achieve highly sensitive cytokine detection (Figure 2C). Specifically, S/B ratios measured in the absence and presence

of 100 nM TNF- $\alpha$  were assessed using biosensors with hybrid membrane coating with ratios ranging from 0:1 (100% RBC) to 1:0 (100% macrophage), obtaining increasing sensitivity with the increment of the macrophage, which contains the TNF- $\alpha$  receptors because more TNF- $\alpha$ /HRP-Ab conjugates are captured on the sensor surface (Figure 2C). Accordingly, a macrophage/RBC membrane ratio of 3:1 was selected for preparing the TNF- $\alpha$  biosensor, which contained a sufficient amount of TNF- $\alpha$  receptors for detection and enough RBC membrane to prevent nonspecific adsorption, as validated in additional experiments (Figure S3).

**3.2. Characterization of the Hybrid Cell Membrane-Coated Sensor Chip.** To verify vesicle fusion on the gold electrode surface, we obtained dual fluorescence images (Figure 3A). Macrophage and RBC membranes were thus labeled with DiI and DiO, respectively, followed by similar membrane coating procedures, indicating the formation of a highly homogeneous hybrid cell membrane coating on the gold chip. Additionally, SEM characterization further validated the

stable formation of the cell membrane coating by drop casting on bare gold chips (Figure 3B), illustrating a full biomembrane surface coverage when comparing that to the granulated Au-sputtered surface. Such a convenient cell membrane coating method was found suitable for the fabrication of the bioelectronic sensor devices as was confirmed by EIS measurements. In this regard, distinct cell membrane coating methods on gold chips were tested (Figure S4), with drop casting being the most efficient method as was verified by the high charge transfer resistance value obtained (Figure 3C). Following evaluation of the operational characteristics, the reproducibility of the bioelectronic chip's fabrication and TNF- $\alpha$  bioassay protocols was assessed by comparing the chronoamperometric measurements obtained from five independent measurements of 5 nM TNF- $\alpha$  standards (Figure 3D). The relative standard deviation (RSD) of 6.7% obtained from the TNF- $\alpha$  measurements reflected the reliability of the new sensor preparation. To complete the physical characterization of the cell membrane-coated chips, the morphology of the cell membrane coating was studied by AFM analysis (Figure 3E), observing an average thickness of the hybrid membrane coating around 50 nm. Such measurement of the membrane coating roughness demonstrated a homogeneous topography, intrinsic to our hybrid membrane-Au system (Figure S5). Finally, the storage stability of the hybrid membrane-coated chips illustrated promise toward large-scale fabrication capability, aiming at a ready-to-use disposable cytokine screening strip. This characteristic was evaluated by fabricating a batch of cell membrane-coated chips, then storing them at 4 °C and frequently testing the sensors over 12 days. Every test day, 0 and 5 nM TNF- $\alpha$  were run in triplicates in amperometry assays. The sensitivity was estimated as S/B from the averaged measurements, and the variation of the relative sensitivity over time was monitored (Figure S6). These results showed the same batch of sensors can be used for TNF- $\alpha$  detection with a sensitivity greater than 80% of the initial value for at least 9 days after fabrication under the current experimental settings.

**3.3. Analytical Performance of the Hybrid Cell Membrane-Coated Sensor Chip.** Following the optimization of the biomembrane composition, we tested the ability of the resulting hybrid membrane-coated bioelectronic sensor to detect different nanomolar TNF- $\alpha$  concentrations through 10  $\mu$ L sample droplet incubations. The biosensor sensitivity was evaluated first using a PBB medium for incubations by examining the amperometric response to increasing TNF- $\alpha$  concentrations over the low (0–10 nM) nanomolar range. The 20 min incubation in the presence of the HRP-Ab was followed by chronoamperometric detection of the HRP reaction product. Well-defined current signals were recorded for these increasing nanomolar TNF- $\alpha$  concentrations, including a clearly distinguishable amperometric response for the 500 pM addition (Figure 4Ai,ii). A linear response was observed in the corresponding calibration curve ( $R^2 = 0.9913$ ), and a limit of detection (LOD) of 150 pM TNF- $\alpha$  was estimated (Table S1), reaching picomolar levels detection through an attractive analytical performance based on fast 1-step 20 min bioassays. Moreover, to evaluate further the rapid binding of TNF- $\alpha$  to the biomembrane, we tested the membrane sensor with two variations: performing a short incubation period for binding of TNF- $\alpha$  between biomembrane and HRP-Ab (about 5 min) and a wide-ranging concentration of TNF- $\alpha$  from 0 to 40 nM. Stable

amperometric signals were observed for each concentration, including a distinct signal change for 5 nM TNF- $\alpha$  from the blank (Figure 4Aiii,iv). In this case, from the constructed calibration curve ( $R^2 = 0.9985$ ), we estimated a LOD of 700 pM, confirming that the cell membrane-based sensor could rapidly capture TNF- $\alpha$  and produce measurable signals in a short period of 5 min. Comparing the analytical characteristics achieved for the 5 min versus the 20 min incubation-based assays, a reasonable 4-fold reduction in sensitivity and corresponding widening of the linear TNF- $\alpha$  concentration range were obtained (Table S1). These findings suggest the possibility of tailoring the analytical parameters of the cell membrane-based biosensor by controlling the incubation time of the sample to the bioreceptors, similar to what has been employed previously for affinity-based electrochemical sensors.<sup>30–32</sup>

For the cell membrane-based sensor chips, the binding efficiency of the membrane receptors is critical for the selective detection of specific cytokines, and it could be influenced by other cytokines and biomolecules present in complex biological samples. To evaluate the selectivity of the sensor for TNF- $\alpha$  detection, the impact on the amperometric signals due to the presence of other cytokines was examined. IL-6 was initially used as the interfering cytokine. The IL-6/TNF- $\alpha$  ratio was varied in the spiked buffer sample, and 100 nM concentration increments of IL-6 were taken into the analysis. Interestingly, the 100 nM TNF- $\alpha$  response was consistent with the 100 nM IL-6 spiked sample (Figure 4Bi). Furthermore, an overall RSD value of 3.4% was obtained for the averaged currents measured for 100 nM TNF- $\alpha$  alone and in the presence of 100 nM increments of IL-6 (Figure 4Bii), with a maximum relative signal variation of 6%. These data confirmed that the biomembrane had sufficient TNF- $\alpha$  binding sites and that the response was not affected by the presence of high IL-6 concentrations. To further establish the selectivity of the biomembrane, we investigated the detection of TNF- $\alpha$  with other cytokines individually (using the same concentration ratio) or in mixtures (tripling the ratio) using IL-6, IL-10, and IFN- $\lambda$ . The resulting 100 nM TNF- $\alpha$  response was not affected by the presence of these additional cytokines (Figure 4Biii). Importantly, in the presence of all cytokines, the signal response was restored for TNF- $\alpha$ , indicating that the binding of TNF- $\alpha$  to the biomembrane was not impaired at the tested concentration. The overall RSD value of 2.4% obtained for the current signals measured for the individual mixing of other cytokines with TNF- $\alpha$  and all together, with a maximum relative signal variation of 5%, confirmed that the selective detection of TNF- $\alpha$  cytokine could be achieved in the multicytokine sample matrix (Figure 4Biv). These findings were in agreement with early reports on cytokine–receptor interactions.<sup>33,34</sup>

The use of the specific detection antibody and standard HRP-TMB system enhanced the sensitivity of the biomembrane sensor. The analytical performance of the cell membrane-based bioelectronic chip for the sensitive detection of various TNF- $\alpha$  concentrations in the presence of IL-6 cytokine was also studied. Here, the current response was measured for wide-ranging low nanomolar TNF- $\alpha$  concentrations in the presence of a constant IL-6 concentration using 20-min incubations along with the HRP-tagged anti-TNF- $\alpha$  antibody. The presence of a high concentration of 50 nM IL-6 did not impair the TNF- $\alpha$  interaction with the TNF $\alpha$ R1 receptors on the membrane surface, leading to sensitive

detection of TNF- $\alpha$  (Figure 4Cii). Well-defined increasing current signals were observed for increasing TNF- $\alpha$  concentrations, leading to a defined TNF- $\alpha$  calibration curve in the presence of 50 nM IL-6. Note that such analytical performance was similar to that observed for TNF- $\alpha$  alone (Figure 4Ai) (Table S2). Interestingly, the sensitivity was retained even in the presence of high 100 nM IL-6 concentration (Figure S7A), but not in the presence of 200 nM IL-6 (Figure S7B). This indicates that detection of a wide range of nanomolar concentrations of TNF- $\alpha$  cytokine could be attained without being influenced by the presence of IL-6 cytokine unless the IL-6 concentration exceeded an upper limit. We hypothesized that abundant protein load on the membrane surface would reduce the accessibility of binding sites for TNF- $\alpha$  and thus the sensitivity of the sensor would decrease (Table S2) (Figure S8). Finally, to evaluate the TNF- $\alpha$  detection capability of the cell membrane-based bioelectronic chip in a sample of superior complexity and thus to examine its potential usability as a biosensor device in real biological matrices, we proceeded to expose the cell membrane-coated electrodes to half diluted human serum spiked with different concentrations of TNF- $\alpha$  from 0 to 250 nM for 20 min. As shown in Figure 4D, the concentration-dependent current changes were stable over the entire range tested so that serum interferents did not prevent effective binding of TNF- $\alpha$  to the biomembrane even for a low concentration of 2.5 nM of TNF- $\alpha$ . The achieved calibration from 2.5 to 50 nM TNF- $\alpha$  yielded a current slope that increased with increasing concentration of TNF- $\alpha$  ( $R^2 = 0.9895$ ) from which a LOD of 1.6 nM was estimated (Table S3). Variations in the analytical performance, regarding linearity interval and sensitivity, compared to that for the analysis of buffer solutions can be attributed to the serum matrix effects on the gold electrode surface. Additional experiments using bare gold chips confirmed the specificity of the amperometric response of the cell membrane coated bioelectronic chips in human serum fluids (Figure S9), supporting further that the biomembrane-based TNF- $\alpha$  detection could be performed in relevant clinical samples with sufficient selectivity, sensitivity, and minimal serum biofouling.

#### 4. CONCLUSIONS

We have demonstrated the use of natural cell membranes as recognition layers to construct biomembrane-coated electrochemical transducers as bioelectronic affinity sensors for highly specific, sensitive, and rapid detection of TNF- $\alpha$  cytokine. Such an attractive bioelectronic platform relies on the coupling of intrinsic recognition and binding of the target cytokine by natural membrane receptors along with amperometric signal transduction. This results in a simple single incubation-based sandwich-like format sensor that represents a unique alternative to conventional immunosensors. The favorable analytical performance with distinct amperometric signals to different TNF- $\alpha$  trace levels, in complex body fluids or in the presence of highly concentrated multicytokine environments. These data suggest that the integrity and functionality of the TNF- $\alpha$  receptors expressed on the macrophage membrane, along with the antifouling properties imparted by the RBC membrane component are well retained during the sensor preparation process. These features allow us to carry out ultrasensitive, selective, and highly efficient TNF- $\alpha$  antigen recognition and feasible sandwich assay performance in  $\leq 20$  min sample incubations. The diversity and distinct function-

alities of different cell types offer considerable promise for developing a variety of biomimetic sensing platforms with a broad range of applications. Various techniques have been developed to enrich membrane receptors.<sup>35</sup> The use of these modified membranes may further improve the kinetics of ligand binding and reduce the incubation time. Such use of natural cell membrane recognition layers for creating a powerful bioaffinity sensing approach paves the way to a new realm of biosensor applications toward the detection of a wide variety of biomarkers.

#### ■ ASSOCIATED CONTENT

##### SI Supporting Information

The Supporting Information is available free of charge at <https://pubs.acs.org/doi/10.1021/jacs.2c07956>.

Instrumentation and reagents employed, analytical characteristics data tables, bioassay protocol schematics, capability of the RBC membrane to prevent nonspecific protein adsorption, capability of the RBC membrane and the hybrid cell membrane to control nonspecific adsorptions, optimization of the cell membrane-based gold electrodes coating protocol, AFM analysis, storage stability of the cell membrane-coated bioelectronic chips, TNF- $\alpha$  calibrations in buffer solutions in presence of high IL-6 levels, effect of the levels of IL-6 on the TNF- $\alpha$  bioassay sensitivity, and specificity of the cell membrane coated sensors in the analysis of serum samples (PDF)

#### ■ AUTHOR INFORMATION

##### Corresponding Authors

Liangfang Zhang – Department of NanoEngineering and Chemical Engineering Program, University of California San Diego, La Jolla, California 92093, United States;  
ORCID: [orcid.org/0000-0003-0637-0654](https://orcid.org/0000-0003-0637-0654); Email: [zhang@ucsd.edu](mailto:zhang@ucsd.edu)

Joseph Wang – Department of NanoEngineering and Chemical Engineering Program, University of California San Diego, La Jolla, California 92093, United States;  
ORCID: [orcid.org/0000-0002-4921-9674](https://orcid.org/0000-0002-4921-9674); Email: [josephwang@ucsd.edu](mailto:josephwang@ucsd.edu)

##### Authors

Eva Vargas – Department of NanoEngineering and Chemical Engineering Program, University of California San Diego, La Jolla, California 92093, United States

Fangyu Zhang – Department of NanoEngineering and Chemical Engineering Program, University of California San Diego, La Jolla, California 92093, United States;  
ORCID: [orcid.org/0000-0002-6522-5230](https://orcid.org/0000-0002-6522-5230)

Amira Ben Hassine – Department of NanoEngineering and Chemical Engineering Program, University of California San Diego, La Jolla, California 92093, United States

Victor Ruiz-Valdepeñas Montiel – Department of NanoEngineering and Chemical Engineering Program, University of California San Diego, La Jolla, California 92093, United States

Rodolfo Mundaca-Uribe – Department of NanoEngineering and Chemical Engineering Program, University of California San Diego, La Jolla, California 92093, United States

Ponnusamy Nandhakumar – Department of NanoEngineering and Chemical Engineering Program,

University of California San Diego, La Jolla, California 92093, United States

Putian He – Department of NanoEngineering and Chemical Engineering Program, University of California San Diego, La Jolla, California 92093, United States

Zhongyuan Guo – Department of NanoEngineering and Chemical Engineering Program, University of California San Diego, La Jolla, California 92093, United States

Zhidong Zhou – Department of NanoEngineering and Chemical Engineering Program, University of California San Diego, La Jolla, California 92093, United States

Ronnie H. Fang – Department of NanoEngineering and Chemical Engineering Program, University of California San Diego, La Jolla, California 92093, United States;  
ORCID: [0000-0001-6373-3189](https://orcid.org/0000-0001-6373-3189)

Weiwei Gao – Department of NanoEngineering and Chemical Engineering Program, University of California San Diego, La Jolla, California 92093, United States

Complete contact information is available at:  
<https://pubs.acs.org/10.1021/jacs.2c07956>

## Author Contributions

The manuscript was written through the contributions of all authors. All authors have given approval to the final version of the manuscript.

## Notes

The authors declare no competing financial interest.

## ACKNOWLEDGMENTS

The Defense Threat Reduction Agency Joint Science and Technology Office for Chemical and Biological Defense (HDTRA1-21-1-0010) supported this work. A.B.H. acknowledges the Fulbright Foreign Student Program for supporting her studies at UC San Diego. All ideas and opinions are of the authors only and do not reflect that of the Fulbright Program.

## REFERENCES

- (1) Liu, Y.; Zhou, Q.; Revzin, A. An Aptasensor for Electrochemical Detection of Tumor Necrosis Factor in Human Blood. *Analyst* **2013**, *138*, 4321–4326.
- (2) Felix, F. S.; Angnes, L. Electrochemical Immunosensors - A Powerful Tool for Analytical Applications. *Biosens. Bioelectron.* **2018**, *102*, 470–478.
- (3) Wen, W.; Yan, X.; Zhu, C.; Du, D.; Lin, Y. Recent Advances in Electrochemical Immunosensors. *Anal. Chem.* **2017**, *89*, 138–156.
- (4) Mehrvar, M.; Bis, C.; Scharer, J. M.; Young, M.; Luong, J. H. Fiber-Optic Biosensors-Trends and Advances. *Anal. Sci.* **2000**, *16*, 677–692.
- (5) Dai, Y.; Liu, C. C. Recent Advances on Electrochemical Biosensing Strategies toward Universal Point-of-Care Systems. *Angew. Chem., Int. Ed.* **2019**, *58*, 12355–12368.
- (6) Pashchenko, O.; Shelby, T.; Banerjee, T.; Santra, S. A Comparison of Optical, Electrochemical, Magnetic, and Colorimetric Point-of-Care Biosensors for Infectious Disease Diagnosis. *ACS Infect. Dis.* **2018**, *4*, 1162–1178.
- (7) Wehmeyer, K. R.; White, R. J.; Kissinger, P. T.; Heineman, W. R. Electrochemical Affinity Assays/Sensors: Brief History and Current Status. *Annu. Rev. Anal. Chem.* **2021**, *14*, 109–131.
- (8) Liu, G.; Wang, S.; Liu, J.; Song, D. An Electrochemical Immunosensor Based on Chemical Assembly of Vertically Aligned Carbon Nanotubes on Carbon Substrates for Direct Detection of the Pesticide Endosulfan in Environmental Water. *Anal. Chem.* **2012**, *84*, 3921–3928.
- (9) Gao, S.; Guisán, J. M.; Rocha-Martin, J. Oriented Immobilization of Antibodies onto Sensing Platforms - A Critical Review. *Anal. Chim. Acta* **2022**, *1189*, 338907.
- (10) Knights, K. M.; Stresser, D. M.; Miners, J. O.; Crespi, C. L. In Vitro Drug Metabolism Using Liver Microsomes. *Curr. Protoc. Pharmacol.* **2016**, *74*, 7.8.1.
- (11) Walgama, C.; Nerimetta, R.; Materer, N. F.; Schildkraut, D.; Elman, J. F.; Krishnan, S. A simple construction of electrochemical liver microsomal bioreactor for rapid drug metabolism and inhibition assays. *Anal. Chem.* **2015**, *87*, 4712–4718.
- (12) Kroll, A. V.; Fang, R. H.; Jiang, Y.; Zhou, J.; Wei, X.; Yu, C. L.; Gao, J.; Luk, B. T.; Dehaini, D.; Gao, W.; Zhang, L. Nanoparticulate Delivery of Cancer Cell Membrane Elicits Multiantigenic Antitumor Immunity. *Adv. Mater.* **2017**, *29*, 1703969.
- (13) Thamphiwatana, S.; Angsantikul, P.; Escajadillo, T.; Zhang, Q.; Olson, J.; Luk, B. T.; Zhang, S.; Fang, R. H.; Gao, W.; Nizet, V.; Zhang, L. Macrophage-Like Nanoparticles Concurrently Absorbing Endotoxins and Proinflammatory Cytokines for Sepsis Management. *Proc. Natl. Acad. Sci. U.S.A.* **2017**, *114*, 11488–11493.
- (14) Wang, S.; Duan, Y.; Zhang, Q.; Komarla, A.; Gong, H.; Gao, W.; Zhang, L. Drug Targeting via Platelet Membrane-Coated Nanoparticles. *Small Struct.* **2020**, *1*, 2000018.
- (15) Hu, C. M.; Zhang, L.; Aryal, S.; Cheung, C.; Fang, R. H.; Zhang, L. Erythrocyte Membrane-Camouflaged Polymeric Nanoparticles as A Biomimetic Delivery Platform. *Proc. Natl. Acad. Sci. U.S.A.* **2011**, *108*, 10980–10985.
- (16) Esteban-Fernández de Avila, B.; Gao, W.; Karshalev, E.; Zhang, L.; Wang, J. Cell-Like Micromotors. *Acc. Chem. Res.* **2018**, *51*, 1901–1910.
- (17) Gao, C.; Lin, Z.; Lin, X.; He, Q. Cell Membrane-Camouflaged Colloid Motors for Biomedical Applications. *Adv. Ther.* **2018**, *1*, 1800056.
- (18) Zhang, F.; Mundaca-Uribe, R.; Askarinam, N.; Li, Z.; Gao, W.; Zhang, L.; Wang, J. Biomembrane-Functionalized Micromotors: Biocompatible Active Devices for Diverse Biomedical Applications. *Adv. Mater.* **2022**, *34*, 2107177.
- (19) Wang, D.; Gao, C.; Zhou, C.; Lin, Z.; He, Q. Leukocyte Membrane-Coated Liquid Metal Nanoswimmers for Actively Targeted Delivery and Synergistic Chemophotothermal Therapy. *Research* **2020**, *2020*, 3676954.
- (20) Gao, J.; Chu, D.; Wang, Z. Cell Membrane-Formed Nanovesicles for Disease-Targeted Delivery. *J. Controlled Release* **2016**, *224*, 208–216.
- (21) Gong, H.; Chen, F.; Huang, Z.; Gu, Y.; Zhang, Q.; Chen, Y.; Zhang, Y.; Zhuang, J.; Cho, Y. K.; Fang, R. H.; Gao, W.; Xu, S.; Zhang, L. Biomembrane-Modified Field Effect Transistors for Sensitive and Quantitative Detection of Biological Toxins and Pathogens. *ACS Nano* **2019**, *13*, 3714–3722.
- (22) Arjuman, A.; Chandra, N. C. Differential Pro-Inflammatory Responses of TNF-Alpha Receptors (TNFR1 and TNFR2) on LOX-1 Signalling. *Mol. Biol. Rep.* **2015**, *42*, 1039–1047.
- (23) Chanput, W.; Mes, J. J.; Wichers, H. J. THP-1 Cell Line: An in Vitro Cell Model for Immune Modulation Approach. *Int. Immunopharmacol.* **2014**, *23*, 37–45.
- (24) Zhang, Q.; Zhou, J.; Zhou, J.; Fang, R. H.; Gao, W.; Zhang, L. Lure-and-Kill Macrophage Nanoparticles Alleviate the Severity of Experimental Acute Pancreatitis. *Nat. Commun.* **2021**, *12*, 4136.
- (25) Vargas, E.; Povedano, E.; Krishnan, S.; Teymourian, H.; Tehrani, F.; Campuzano, S.; Dassau, E.; Wang, J. Simultaneous Cortisol/Insulin Microchip Detection Using Dual Enzyme Tagging. *Biosens. Bioelectron.* **2020**, *167*, 112512.
- (26) Paciotti, G. F.; Myer, L.; Weinreich, D.; Goia, D.; Pavel, N.; McLaughlin, R. E.; Tamarkin, L. Colloidal Gold: A Novel Nanoparticle Vector for Tumor Directed Drug Delivery. *Drug Deliv.* **2004**, *11*, 169–183.
- (27) Tsai, D. H.; Davila-Morris, M.; DelRio, F. W.; Guha, S.; Zachariah, M. R.; Hackley, V. A. Quantitative Determination of Competitive Molecular Adsorption on Gold Nanoparticles Using

Attenuated Total Reflectance-Fourier Transform Infrared Spectroscopy. *Langmuir* **2011**, *27*, 9302–9313.

(28) Tsai, D. H.; DelRio, F. W.; Keene, A. M.; Tyner, K. M.; MacCuspie, R. I.; Cho, T. J.; Zachariah, M. R.; Hackley, V. A. Adsorption and Conformation of Serum Albumin Protein on Gold Nanoparticles Investigated Using Dimensional Measurements and in Situ Spectroscopic Methods. *Langmuir* **2011**, *27*, 2464–2477.

(29) Tsai, D. H.; Elzey, S.; DelRio, F. W.; Keene, A. M.; Tyner, K. M.; Clogston, J. D.; MacCuspie, R. I.; Guha, S.; Zachariah, M. R.; Hackley, V. A. Tumor Necrosis Factor Interaction with Gold Nanoparticles. *Nanoscale* **2012**, *4*, 3208–3217.

(30) Rath, D.; Panda, S. Correlation of Capture Efficiency with the Geometry, Transport, and Reaction Parameters in Heterogeneous Immunosensors. *Langmuir* **2016**, *32*, 1410–1418.

(31) Vargas, E.; Torrente-Rodríguez, R. M.; Ruiz-Valdepeñas Montiel, V.; Povedano, E.; Pedrero, M.; Montoya, J. J.; Campuzano, S.; Pingarrón, J. M. Magnetic Beads-Based Sensor with Tailored Sensitivity for Rapid and Single-Step Amperometric Determination of miRNAs. *Int. J. Mol. Sci.* **2017**, *18*, 2151.

(32) Zorea, J.; Shukla, R. P.; Elkabets, M.; Ben-Yoav, H. Probing Antibody Surface Density and Analyte Antigen Incubation Time as Dominant Parameters Influencing the Antibody-Antigen Recognition Events of a Non-Faradaic and Diffusion-Restricted Electrochemical Immunosensor. *Anal. Bioanal. Chem.* **2020**, *412*, 1709–1717.

(33) Kitaura, H.; Marahleh, A.; Ohori, F.; Noguchi, T.; Nara, Y.; Pramusita, A.; Kinjo, R.; Ma, J.; Kanou, K.; Mizoguchi, I. Role of the Interaction of Tumor Necrosis Factor-Alpha and Tumor Necrosis Factor Receptors 1 and 2 in Bone-Related Cells. *Int. J. Mol. Sci.* **2022**, *23*, 1481.

(34) Suo, F.; Zhou, X.; Setiroikromo, R.; Quax, W. J. Receptor Specificity Engineering of TNF Superfamily Ligands. *Pharmaceutics* **2022**, *14*, 181.

(35) Ai, X.; Wang, S.; Duan, Y.; Zhang, Q.; Chen, M. S.; Gao, W.; Zhang, L. Emerging Approaches to Functionalizing Cell Membrane-Coated Nanoparticles. *Biochemistry* **2021**, *60*, 941–955.

CAS BIOFINDER DISCOVERY PLATFORM™

**ELIMINATE DATA SILOS. FIND WHAT YOU NEED, WHEN YOU NEED IT.**

A single platform for relevant, high-quality biological and toxicology research

Streamline your R&D

**CAS**  
A division of the  
American Chemical Society